
Article:
Smith, G.N., Canning, S., Derry, M.J. et al. (3 more authors) (2020) Influence of an ionic comonomer on polymerization-induced self-assembly of diblock copolymers in non-polar media. Polymer Chemistry, 11 (14). pp. 2605-2614. ISSN 1759-9954

https://doi.org/10.1039/d0py00101e

Polymer Chemistry

Accepted Manuscript

This article can be cited before page numbers have been issued, to do this please use: G. N. Smith, S. Canning, M. J. Derry, O. O. Mykhaylyk, S. E. Youngs and S. P. Armes, *Polym. Chem.*, 2020, DOI: 10.1039/D0PY00101E.

ROYAL SOCIETY OF CHEMISTRY

rsc.li/polymers

View Article Online
DOI: 10.1039/D0PY00101E

Cite this: DOI: 00.0000/xxxxxxxxxx

Influence of an ionic comonomer on polymerization-induced self-assembly of diblock copolymers in non-polar media†

Gregory N. Smith,*[ab] Sarah L. Canning,[a‡] Matthew J. Derry,[a§] Oleksandr O. Mykhaylyk,[a] Sarah E. Norman,[c¶] and Steven P. Armes*[a]

Received Date
Accepted Date

DOI: 00.0000/xxxxxxxxxx

A series of poly(stearyl methacrylate)–poly(benzyl methacrylate) (PSMA–PBzMA) diblock copolymer nano-objects has been synthesized via reversible addition–fragmentation chain-transfer (RAFT) dispersion polymerization in *n*-dodecane at 20 wt. %. This polymerization-induced self-assembly (PISA) formulation was modified by the incorporation of an anionic monomer, tetradodecylammonium 3-sulfopropyl methacrylate ($[NDod_4]^+[SPMA]^-$) into the oil-insoluble PBzMA block. According to the literature (M. J. Derry *et al.*, *Chem. Sci.*, 2016, **7**, 5078–5090), $PSMA_{18}$–PBzMA diblock copolymers only form spheres using this formulation for any core DP. Unexpectedly, incorporating just a small fraction (< 6 mole %) of $[NDod_4]^+[SPMA]^-$ comonomer into the structure-directing block resulted in the formation of non-spherical diblock copolymer nano-objects, including pure worm-like and vesicular morphologies. However, only spherical micelles could be formed using a longer $PSMA_{34}$ stabilizer. These diblock copolymer nano-objects were characterized by transmission electron microscopy, small-angle X-ray scattering, and dynamic light scattering. The bulky nature of the ionic comonomer appears to make it possible to avoid the kinetically-trapped sphere morphology. This study reveals a new approach for tuning the morphology of diblock copolymer nano-objects in non-polar media.

1 Introduction

AB diblock copolymers are well-known to undergo self-assembly in selective solvents to form polymer micelles.[1] Pioneering work by Eisenberg and others demonstrated that various amphiphilic diblock copolymers can form a wide range of morphologies when slowly transferred from water-miscible organic solvents into aqueous solution.[2–4] Unfortunately, such post-polymerization processing is usually performed at relatively low copolymer concentrations,[2,4] which severely limits potential commercial applications. Nevertheless, systematic variation of the mean degree of polymerization (DP) of each block enabled the rational preparation of a desired copolymer morphology (such as spheres, cylinders, or vesicles).[4] The preferred copolymer morphology can be understood by considering the packing parameter (P), which is a geometric relationship for amphiphiles that links the core volume (v), the core chain length (l_c), and the projected surface area (a_0), as shown in Equation 1.[5,6]

$$P = \frac{v}{a_0 l_c} \quad (1)$$

This dictates the self-assembly of amphiphiles, such as surfactants or block copolymers.

Over the past decade, polymerization-induced self-assembly (PISA) has become widely recognized as an efficient and highly attractive means of preparing diblock copolymer nano-objects directly at high concentrations, particularly when coupled with reversible addition–fragmentation chain-transfer (RAFT) polymerization.[7–15] In a PISA synthesis, a soluble precursor block is chain-extended using a second monomer, initially forming a soluble diblock copolymer. At a critical DP, the growing second block becomes insoluble, resulting in the spontaneous *in situ* formation of self-assembled diblock copolymer nano-objects.

[a] *Department of Chemistry, University of Sheffield, Brook Hill, Sheffield, South Yorkshire, S3 7HF, United Kingdom. E-mail: s.p.armes@sheffield.ac.uk*
[b] *Niels Bohr Institute, University of Copenhagen, H. C. Ørsted Institute, Universitetsparken 5, 2100 Copenhagen Ø, Denmark. E-mail: gregory.smith@nbi.ku.dk*
‡ *Current address: Fujifilm Speciality Ink Systems Ltd, Pysons Road, Broadstairs, Kent CT10 2LE, United Kingdom.*
§ *Current address: School of Engineering & Applied Science, Aston University, Birmingham, United Kingdom.*
[c] *School of Chemistry and Chemical Engineering, The QUILL Centre, Queen's University Belfast, Belfast BT9 5AG, United Kingdom*
¶ Current address: ISIS-STFC, Rutherford Appleton Laboratory, Chilton, Oxon, OX11 0QX, United Kingdom.
† Electronic Supplementary Information (ESI) available: Information on anionic comonomer synthesis, SAXS models and fitting, and DLS size distributions. See DOI: 00.0000/00000000.

View Article Online
DOI: 10.1039/D0PY00101E

The packing parameter concept can be used to account for the self-assembly behavior of amphiphilic poly(glycerol monomethacrylate)–poly(2-hydroxypropyl methacrylate) (PGMA–PHPMA) diblock copolymers to form spheres, worms, or vesicles in aqueous media.[8,16,17] The copolymer morphology was found to be independent of the copolymer concentration when using a relatively short PGMA stabilizer for the polymerization of HPMA. However, when a longer PGMA block was used, the final copolymer morphology depended on the copolymer concentration. More specifically, kinetically-trapped spheres are typically observed at lower copolymer concentrations. Similar effects have been observed for syntheses performed in either polar solvents[18] or non-polar solvents.[11,19,20] The formation of kinetically-trapped spheres can be rationalized by considering the effectiveness of the steric stabilizer. If the soluble precursor block is relatively long, then this leads to effective steric stabilization,[21] which in turn prevents sphere-sphere fusion from occurring during PISA. If this initial fusion event does not occur, then worm-like micelles, which are believed to form from the result of multiple one-dimensional sphere-sphere fusion events, cannot be formed. Ultimately, this means that vesicles cannot be accessed either, since their formation evolves from worm-like micelles via branched worms, octopuses, and jellyfishes.[22] Thus, using relatively long steric stabilizer blocks invariably leads to the formation of spheres. Over the last decade, various core-forming blocks, such as, poly(methyl acrylate),[23–25] poly(benzyl methacrylate),[19,20,26–33] poly(3-phenylpropyl methacrylate),[34–36] poly(benzyl acrylate),[37] poly(*N*-2-(methacryloyloxy)ethyl pyrrolidone),[38] poly(phenyl acrylate),[39] poly(2,2,2-trifluoroethyl methacrylate),[40,41] and poly(glycidyl methacrylate)[42] have been reported for PISA syntheses conducted in non-polar solvents. In the present study, we revisit one of these established PISA formulations: poly(stearyl methacrylate)–poly(benzyl methacrylate) (PSMA–PBzMA or S–P(Bz)) diblock copolymer nano-objects in *n*-dodecane. As discussed above, the DP of the oil-soluble PSMA precursor block determines whether spherical, worm-like, or vesicular nanoparticles form. For example, a short $PSMA_{13}$ macro-CTA enables access to all three morphologies, whereas longer $PSMA_{18}$ or $PSMA_{31}$ macro-CTAs only lead to spheres, at a copolymer concentration of 20 wt. %.[11] In this study, we focus on synthesizing new diblock copolymer nano-objects using either $PSMA_{18}$ or $PSMA_{34}$ macro-CTAs as the steric stabilizer block. First, RAFT solution polymerization of SMA was conducted in toluene using cumyl dithiobenzoate to produce PSMA macromolecular chain-transfer agents (macro-CTAs), which was followed by purification to remove residual SMA monomer. Then, this oil-soluble precursor block was used for the RAFT dispersion polymerization of BzMA to prepare diblock copolymer nano-objects directly in *n*-dodecane at 90 °C, see Scheme 1(a). This previously reported PISA formulation was then modified by statistical copolymerization of BzMA with tetradodecylammonium 3-sulfopropyl methacrylate ($[NDod_4]^+[SPMA]^-$) to produce new diblock copolymer nano-objects with partially ionic cores, see Scheme 1(b).

Given the low relative permittivity of the *n*-dodecane solvent ($\varepsilon_r \sim 2$), we anticipated that the introduction of an ionic comonomer should have a much more significant impact than for PISA syntheses performed in water.[43] This is the fundamental question that we set out to address in this study. To what extent does the incorporation of an ionic monomer have on the final copolymer morphology in a non-polar solvent?

2 Experimental

2.1 Materials

Stearyl methacrylate (SMA) and benzyl methacrylate (BzMA, 96%) were purchased from Sigma–Aldrich (UK). BzMA monomer was passed over a basic alumina column to remove inhibitor prior to use. 2,2-Azobisisobutyronitrile (AIBN) initiator was purchased from Molekula (UK), and *tert*-butyl peroxy-2-ethylhexanoate (Trigonox S1S or T21S) initiator was a gift from AkzoNobel (The Netherlands). Cumyl dithiobenzoate (CDB, 99%) and *n*-dodecane (UK, ≥99%) were purchased from Sigma–Aldrich (UK) and used a supplied. All precursors for tetradodecylammonium 3-sulfopropylmethacrylate ($[NDod_4]^+[SPMA]^-$) were obtained from Sigma–Aldrich.[44,45] Tetrahydrofuran (THF) and ethanol were purchased from either VWR, Sigma–Aldrich, or Fisher (UK) and were used as supplied. Dichloromethane-d_2, (CD_2Cl_2) was obtained from Cambridge Isotope Laboratories (USA), and chloroform-d_3 ($CDCl_3$) was obtained from Sigma–Aldrich (UK).

2.1.1 Poly(stearyl methacrylate) macromolecular chain transfer agents

Two poly(stearyl methacrylate) (PSMA) macromolecular chain transfer agents (macro-CTAs) were synthesized targeting different DPs. For the RAFT synthesis of $PSMA_{18}$, SMA (20.2465 g, 59.80 mmol), CDB (1.6313 g, 5.99 mmol), AIBN (0.1941 g, 1.18 mol; CDB/AIBN molar ratio = 5.1) were dissolved in toluene (32.7050 g). For the RAFT synthesis of $PSMA_{34}$, SMA (20.0245 g, 59.14 mmol), CDB (0.5791 g, 2.13 mmol), AIBN (0.0699 g, 0.43 mol; CDB/AIBN molar ratio = 5.0) were dissolved in toluene (30.9778 g). The solutions were purged with nitrogen and then heated at 70 °C for 10 h. Each SMA polymerization proceeded to ~ 75% conversion, and the resulting crude PSMA macro-CTAs were purified by precipitation into ethanol. The purified PSMA were characterized using size exclusion chromatography (SEC) with THF eluent with low dispersity poly(methyl methacrylate) calibration standards to assess their molar mass distributions (both dispersity, $Đ_M = M_w/M_n$, and standard deviation, σ)[46,47] and by ^{1}H NMR spectroscopy in CD_2Cl_2 to determine their mean DP (by comparing the integrated aromatic protons at 7.1–8.1 ppm assigned to the RAFT end-groups with the two oxymethylene protons assigned to the polymerized SMA repeat units at 3.8–4.0 ppm). The number-average molar mass (M_n) and dispersities ($Đ_M$) from SEC were found to be $M_n = 7.8$ kg mol^{-1} and $Đ_M = 1.14$ for $PSMA_{18}$ and $M_n = 13.2$ kg mol^{-1} and $Đ_M = 1.14$ for $PSMA_{34}$. Using the DP determined from NMR and the dispersity determined from SEC,[47] the DP and standard deviations were calculated to be 18 ± 7 for $PSMA_{18}$ and 34 ± 13 for $PSMA_{34}$. The dispersity ($Đ$) can be related to the standard devia-

View Article Online
DOI: 10.1039/D0PY00101E

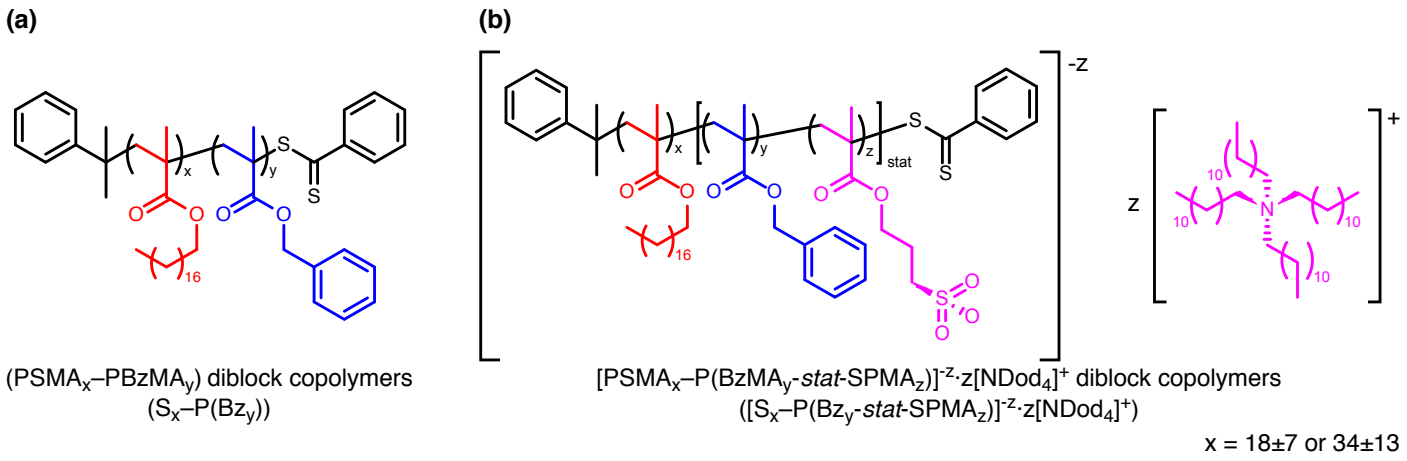

Scheme 1 Copolymers used in this study. (a) Poly(stearyl methacrylate)–poly(benzyl methacrylate) (PSMA–PBzMA or S–P(Bz)) diblock copolymers. (b) Partially anionic [poly(stearyl methacrylate)–poly((benzyl methacrylate)-*stat*-(3-sulfopropyl methacrylate))]$^-$ diblock copolymers with tetradodecylammonium counterions (([PSMA–P(BzMA-*stat*-SPMA)]$^-$ · [NDod$_4$]$^+$) or ([S–P(Bz-*stat*-SPMA)]$^-$ · [NDod$_4$]$^+$)).

tion (σ) and the mean (μ) using the Equation 2.[47]

$$Đ = 1 + \frac{\sigma^2}{\mu^2} \quad (2)$$

2.1.2 Anionic comonomer

Tetradodecylammonium 3-sulfopropylmethacrylate ([NDod$_4$]$^+$[SPMA]$^-$) was prepared via an ion exchange reaction using halide salt precursors, as reported in the literature,[44,45] shown in the ESI (Scheme S1)†. Briefly, tetradodecylammonium bromide was first converted into the corresponding chloride salt via ion exchange by dissolving the bromide salt in water and then running this aqueous solution through a column packed with Amberlite IRA-400 (Cl) resin. The resulting tetradodecylammonium chloride salt was dissolved in acetonitrile, and an aqueous solution of potassium 3-sulfopropylmethacrylate (K$^+$[SPMA]$^-$) was added dropwise. The suspension was stirred overnight, filtered, and then the solvent was removed under vacuum. The solid residues were then dissolved in dichloromethane, filtered, and the solvent removed under vacuum. This protocol was repeated three times to remove all residual KCl salt, resulting in the purified [NDod$_4$]$^+$[SPMA]$^-$ salt. The purity of the monomer was confirmed by elemental analysis. (Found: C, 74.2%; H, 11.6%; N, 1.6%. Calc. for $C_{55}H_{111}NO_5S$: C, 73.5%; H, 12.5%; N, 1.6%.)

2.1.3 PSMA–PBzMA (S–P(Bz)) and PSMA–P(BzMA-*stat*-SPMA) ([S–P(Bz$_y$-*stat*-SPMA$_z$)]$^{-z}$ · z[NDod$_4$]$^+$) block copolymers

Multiple series of PSMA$_x$–PBzMA$_y$ and [PSMA$_{18}$–P(BzMA$_y$-*stat*-SPMA$_z$)]$^{-z}$ · z[NDod$_4$]$^+$ diblock copolymer nano-objects were synthesized using either a PSMA$_{18}$ or PSMA$_{34}$ macro-CTA (Scheme 1).[28,29] The PSMA macro-CTA, BzMA, [NDod$_4$]$^+$[SPMA]$^-$, and T21S initiator (added as a 10% solution in *n*-dodecane; macro-CTA/T21S molar ratio = 3.0) were dissolved in *n*-dodecane at the desired concentration. The reaction mixture was degassed using nitrogen for 30 min at ambient temperature and then heated to 90 °C, with the polymerization reaction allowed to proceed for at least 18 h. Each copolymer was analyzed using ^{1}H NMR spectroscopy in $CDCl_3$ to calculate the final comonomer conversion, overall DP, and mole fraction of incorporated comonomer. In addition, each PSMA$_x$–PBzMA$_y$ diblock copolymer was analyzed by SEC (THF eluent with low-dispersity poly(methyl methacrylate) calibration standards). For a block copolymer, the dispersity ($Đ$) can be calculated from the dispersities ($Đ_i$) and mean DPs (μ_i) of each of the blocks ($i \in \{1,2\}$), as shown in Equation 3.[47]

$$Đ_{1+2} = 1 + \frac{\mu_1^2\,(Đ_1 - 1) + \mu_2^2\,(Đ_2 - 1)}{(\mu_1 + \mu^2)^2} \quad (3)$$

Characterizations of these diblock copolymers and nano-objects are given in Tables 1, 2, and 3.

2.2 Methods

2.2.1 Transmission electron microscopy (TEM)

Diblock copolymer dispersions were diluted with *n*-dodecane to produce 0.01 wt. % dispersions. Copper TEM grids (Agar Scientific, UK) were sputter-coated in-house with a thin film of amorphous carbon. For each diblock copolymer dispersion, an individual droplet was placed onto a carbon-coated TEM grid, and the solvent was allowed to evaporate at ambient temperature. To stain the deposited nanoparticles, the grids were exposed to ruthenium(IV) oxide vapor for 7 min at 20 °C prior to analysis.[19] This heavy metal compound acted as a positive stain to improve contrast. The ruthenium(IV) oxide was prepared as follows: ruthenium(II) oxide (0.30 g) was added to water (50 g) to form a black slurry; addition of sodium periodate (2.0 g) with stirring produced a yellow solution of ruthenium(IV) oxide within 1 min. Imaging was performed at 100 kV using a Phillips CM100 instrument equipped with a Gatan 1k CCD camera.

2.2.2 Small-angle X-ray scattering (SAXS)

Small-angle X-ray scattering (SAXS) measurements were performed using two instruments: the beamline I22 at Diamond Light Source (Didcot, UK) and the beamline ID02 at the ESRF

View Article Online
DOI: 10.1039/D0PY00101E

Table 1 Summary of characterizations of PSMA–PBzMA diblock copolymers and nano-objects

PBzMA DP[(a)]	wt. %[(b)]	Conversion[(a)] / %	M_n PBzMA[(c)] / (kg mol^{-1})	$Đ_M(M_w/M_n)$ PBzMA[(c,d)]	σ PBzMA DP[(d)]	d_Z[(e)] / nm	Polydispersity index[(e)]
$PSMA_{18}$–$PBzMA_y$							
48	20	97	6.3	1.46	33	21	0.02
95	20	96	17.4	1.33	55	34	0.04
98	30	98	17.7	1.29	53	42	0.08
97	40	97	22.6	2.49	118	198	0.22
196	20	97	37.3	1.33	112	54	0.03
202	30	98	37.3	1.26	104	87	0.07
196	40	97	45.1	2.56	244	242	0.07
295	20	97	53.5	1.32	167	72	0.03
295	30	97	55.4	1.29	158	189	0.21
299	40	97	52.6	4.15	530	413	0.12
$PSMA_{34}$–$PBzMA_y$							
96	20	96	16.7	1.59	74	33	0.09
101	30	97	18.0	1.52	73	32	0.02
97	40	97	18.1	1.63	77	40	0.14
194	20	95	32.6	1.55	145	58	0.17
195	30	98	35.4	1.44	128	49	0.09
197	40	98	36.1	1.40	124	55	0.15
294	20	94	55.9	2.09	307	68	0.06
289	30	98	53.5	1.49	202	61	0.09
292	40	98	55.3	1.45	195	69	0.10

[(a)] Conversion of BzMA determined by ^{1}H NMR in $CDCl_3$
[(b)] Concentration of solid material (PSMA macro-CTA and BzMA monomer) in the reaction
[(c)] Determined by THF SEC (refractive index detector with PMMA calibration standards)
[(d)] Calculated using Harrisson's method as explained in the text[47] ($Đ_M$ $PSMA_{18}$ = 1.14, $Đ_M$ $PSMA_{34}$ = 1.21)
[(e)] Determined by DLS of 0.1 wt. % dispersions in *n*-dodecane at 25 °C

Table 2 Summary of characterizations of $PSMA_{18}$–P(BzMA-*stat*-SPMA) diblock copolymers and nano-objects prepared at 20 wt. % in *n*-dodecane

P(BzMA-*stat*-SPMA) DP[(a)]	Mole fraction PBzMA	Mole fraction PSPMA	Conversion[(a)] / %	d_Z[(b)] / nm	Polydispersity index[(b)]
47	0.9956	0.0044	97	22	0.01
47	0.9796	0.0204	96	22	0.04
48	0.9672	0.0328	96	23	0.06
47	0.9529	0.0471	96	25	0.13
45	0.9374	0.0626	94	443	0.35
74	0.9802	0.0198	97	39	0.12
74	0.9606	0.0394	97	70	0.15
93	0.9893	0.0107	97	88	0.18
104	0.9813	0.0187	98	222	0.52
96	0.9694	0.0306	98	218	0.35
91	0.9604	0.0396	96	227	0.34
99	0.9529	0.0471	96	301	0.53
92	0.9356	0.0644	96	727	0.81
96	0.9313	0.0687	96	505	0.67
99	0.9203	0.0797	95	469	0.69
109	0.9119	0.0881	96	514	0.34
142	0.9806	0.0194	96	131	0.09
124	0.9597	0.0403	96	199	0.21
144	0.9515	0.0485	97	237	0.20
194	0.9951	0.0049	98	56	0.02
179	0.9885	0.0115	97	66	0.02
184	0.9790	0.0210	97	103	0.07
191	0.9708	0.0292	96	164	0.07
191	0.9564	0.0436	97	310	0.19
190	0.9492	0.0508	97	275	0.15
182	0.9399	0.0601	94	396	0.36
193	0.9244	0.0756	96	449	0.12
246	0.9806	0.0194	96	113	0.04
236	0.9509	0.0491	96	313	0.18
264	0.9415	0.0585	96	403	0.04
308	0.9902	0.0098	97	406	0.20
286	0.9799	0.0201	97	167	0.06
318	0.9714	0.0286	97	199	0.03
296	0.9587	0.0413	97	310	0.12
274	0.9504	0.0496	91	391	0.10
283	0.9348	0.0652	94	572	0.12

[(a)] Conversion of BzMA determined by ^{1}H NMR in $CDCl_3$
[(b)] Determined by DLS of 0.1 wt. % dispersions in *n*-dodecane at 25 °C

View Article Online
DOI: 10.1039/D0PY00101E

Table 3 Summary of characterizations of $PSMA_{34}$–P(BzMA-*stat*-SPMA) diblock copolymers and nano-objects prepared at 20 wt. % in *n*-dodecane

P(BzMA-*stat*-SPMA) DP[(a)]	Mole fraction PBzMA	Mole fraction PSPMA	Conversion[(a)] / %	d_Z[(b)] / nm	Polydispersity index[(b)]
95	0.9748	0.0252	96	33	0.02
98	0.9497	0.0503	95	36	0.01
95	0.9366	0.0634	95	36	0.01
96	0.9356	0.0744	95	37	0.03
194	0.9752	0.0248	96	49	0.04
187	0.9487	0.0513	95	51	0.04
194	0.9395	0.0605	96	54	0.03
189	0.9235	0.0765	96	75	0.06
277	0.9749	0.0251	93	60	0.02
290	0.9507	0.0493	96	63	0.02
288	0.9386	0.0614	95	83	0.15
285	0.9262	0.0738	96	127	0.05

[(a)] Conversion of BzMA determined by ^{1}H NMR in $CDCl_3$
[(b)] Determined by DLS of 0.1 wt. % dispersions in *n*-dodecane at 25 °C

(Grenoble, France). Scattering intensity is measured as a function of the modulus of the momentum transfer vector (Q) is defined in Equation 4, where θ is half the scattering angle and λ is the wavelength of the radiation.

$$Q = \frac{4\pi \sin\theta}{\lambda} \quad (4)$$

On I22, monochromatic X-ray radiation (wavelength $\lambda = 1.24$ Å) was used, giving an accessible Q range of $0.0015 < Q < 0.13$ Å^{-1}. Measurements were conducted on 1.0 wt. % copolymer dispersions using a flow-through capillary set-up as the sample holder, with a glass capillary of 2.0 mm diameter. Raw SAXS data were reduced (integration and normalization) using Dawn software supplied by Diamond Light Source[48].

On ID02, monochromatic X-ray radiation ($\lambda = 0.995$ Å) and a Rayonix MX-170HS CCD detector was used to give an accessible Q-range of $3 \times 10^{-4} < Q < 0.08$ Å^{-1}. Two sample-detector distances (6 and 30 m) were used. Glass capillaries of 2.0 mm diameter were used as a sample holder. Scattering data were reduced using standard routines from the beamline and were further analyzed using Irena SAS macros for Igor Pro.[49]

All one-dimensional SAXS data obtained using the above instruments were processed (calibration and background subtractions) using Irena SAS macros for Igor Pro.[49] Data were fitted as described in the text using bespoke models implemented for Irena SAS macros for Igor Pro.[49]

2.2.3 Dynamic light scattering (DLS)

Dynamic light scattering (DLS) measurements were performed at 25 °C using a Malvern Zetasizer Nano ZS (Malvern Instruments, UK). The as-synthesized dispersions of diblock copolymer nano-objects were diluted with *n*-dodecane to obtain concentrations of ~ 0.1 wt. %. Three measurements of typically ten runs of 10 s duration (the exact number was instrument-determined) were averaged. Cumulants analysis was performed to determine the *Z*-average diameter (d_Z) and the polydispersity index for each dispersion.

3 Results

Poly(stearyl methacrylate)–poly(benzyl methacrylate) (PSMA–PBzMA) diblock copolymers prepared by PISA can form sphere, worm, or vesicle morphologies in non-polar media, depending on the precise target diblock copolymer composition. According to Derry *et al.*, only spheres are obtained when using a $PSMA_{18}$ macro-CTA to polymerize BzMA at 20 wt. % in *n*-dodecane.[28] Presumably this is because this steric stabilizer block is already sufficiently large to prevent efficient sphere-sphere fusion under such conditions. Sphere-sphere fusion is the critical first step that is required to access non-spherical morphologies.[8,10] In this study, $PSMA_{18}$–$PBzMA_y$ spheres have been produced using the same PISA formulation, as illustrated by the DLS size distributions and representative TEM micrographs shown in Figure 1.

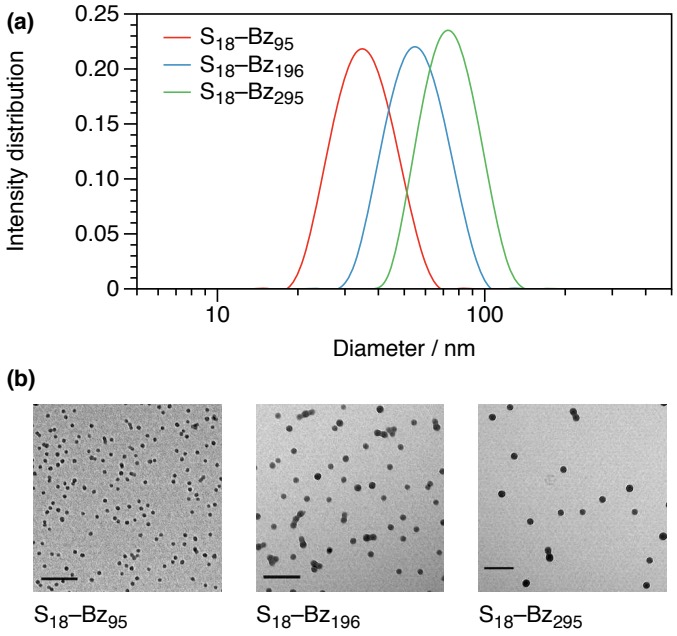

Fig. 1 Characterization obtained for $PSMA_{18}$–$PBzMA_y$ in *n*-dodecane (referred to as S_{18}–Bz_y for brevity) diblock copolymers nano-objects. (a) DLS size distributions and (b) representative TEM micrographs. Scale bars are 200 nm in each case.

For this series of $PSMA_{18}$–$PBzMA_y$ diblock copolymers, only spheres could be obtained regardless of the target DP (y) of the PBzMA block. Thus, the effect of incorporating an anionic comonomer into structure-forming block should be immediately apparent. Accordingly, a suitable oil-soluble ionic comonomer

View Article Online
DOI: 10.1039/D0PY00101E

($[NDod_4]^+[SPMA]^-$) was used to prepare a series of $[PSMA_{18}–P(BzMA_y\text{-}stat\text{-}SPMA_z)]^{-z} \cdot z[NDod_4]^+$ ($[S_{18}–P(Bz_y\text{-}stat\text{-}SPMA_z)]^{-z} \cdot z[NDod_4]^+$) statistical diblock copolymer nano-objects.

3.1 Copolymer morphology

Reproducible targeting of pure copolymer morphologies for PISA formulations generally requires construction of a morphology map.[17,19,20,26,28,50] Typically, such morphology maps indicate the relationship between the steric stabilizer block DP and the structure-directing block DP (at a constant copolymer concentration) or the structure-directing block DP and the copolymer concentration (for a fixed steric stabilizer block DP). However, the morphology map shown in Figure 2 differs from those typically produced for PISA formulations.[10] In this case, the *y*-axis denotes the overall DP for the block copolymer in the nano-object core (the total number of BzMA and SPMA repeat units), and *x*-axis denotes the mole fraction of the ionic comonomer. Both the steric stabilizer block DP (in this case $PSMA_{18}$) and copolymer concentration (20 wt. %) were fixed for the PISA syntheses featured in this morphology map.

Pure spheres, worms, and vesicles can be produced, as would be expected for a typical PISA synthesis, by judiciously selecting an appropriate DP for the structure-directing statistical block and by adjusting the mole fraction of the anionic comonomer. Mixed morphologies are found surrounding all these pure systems. Additionally, large and ill-defined compound micelles are also observed. The term "compound micelles" has been used in the literature previously to describe instances where short stabilizers can no longer maintain colloidal stability and the growing micelles fuse together.[51,52] We emphasize that only kinetically-trapped spheres are obtained when using this same $PSMA_{18}$ macro-CTA for PISA syntheses conducted under identical conditions in the absence of anionic comonomer. For example, the three diblock copolymer nano-objects shown in Figure 1 form only spheres, and they fall along the *y*-axis (mole fraction of anionic comonomer of 0) in Figure 2. Similarly, if the mole fraction of anionic comonomer is too low or if the DP of the structure-directing block is too short, then only spheres are obtained. For anionic comonomer mole fractions ranging between ~ 0.02 and ~ 0.06, either pure spheres, worms, or vesicles are formed as the DP of the structure-directing block is systematically increased. Each of these pure morphologies is bounded by one or more mixed regions.

Copolymer morphologies were assessed by visual inspection of the dispersions, dynamic light scattering, and transmission electron microscopy. Additionally, small-angle X-ray scattering (SAXS) measurements were performed to obtain more robust information about the morphologies. The technique does not suffer from sampling bias, as the scattering from a system-average number of particles is detected. Figure 3 shows SAXS data for samples of pure spheres, worms, and vesicles. These data were fitted to appropriate models for each morphology, which is discussed in the ESI.† These data supported our initial assessment of the morphologies and confirm that pure spheres, worms, and vesicles can be obtained by systematic variation of the overall DP

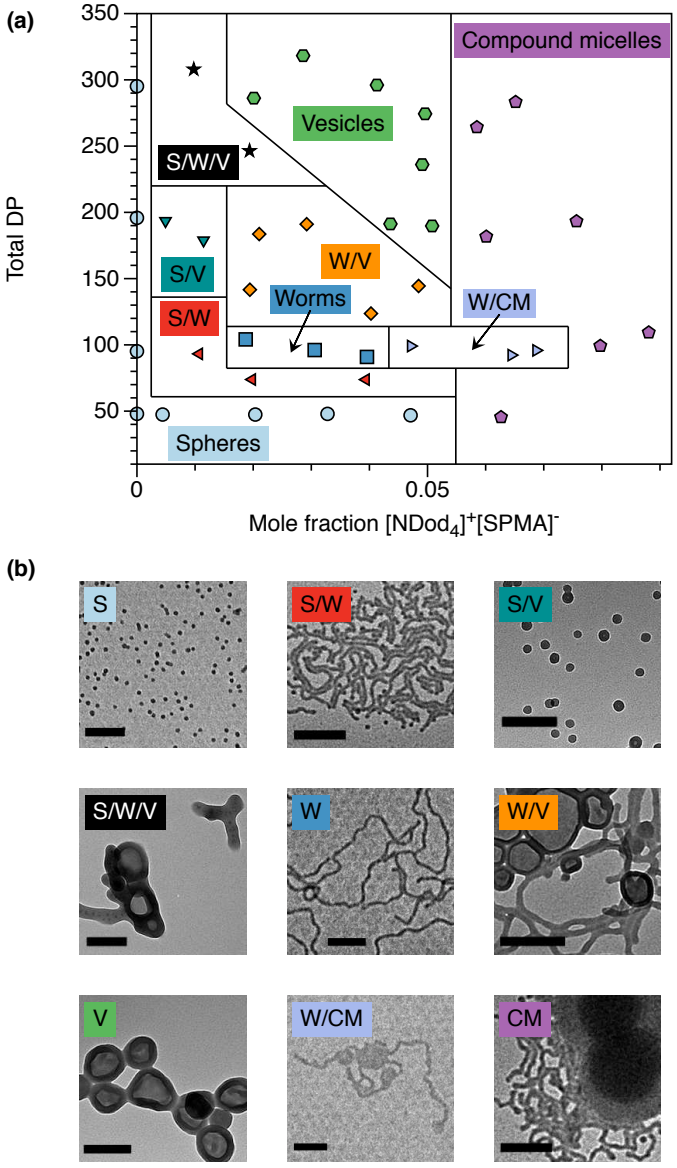

Fig. 2 Various copolymer morphologies formed by $[PSMA_{18}–P(BzMA_y\text{-}stat\text{-}SPMA_z)]^{-z} \cdot z[NDod_4]^+$ diblock copolymer nano-objects synthesized by PISA in *n*-dodecane at a copolymer concentration of 20 wt. %. (a) Morphology map showing the total structure-directing block DP (total number of BzMA and SPMA repeat units) as the *y*-axis and the mole fraction of the anionic comonomer as the *x*-axis. (b) Representative TEM micrographs of all types of copolymer morphologies shown in (a). Scale bars are 200 nm in each case. (S = spheres, W= worms, V = vesicles, CM = compound micelles.)

View Article Online
DOI: 10.1039/D0PY00101E

of the structure-directing block and the mole fraction of anionic comonomer.

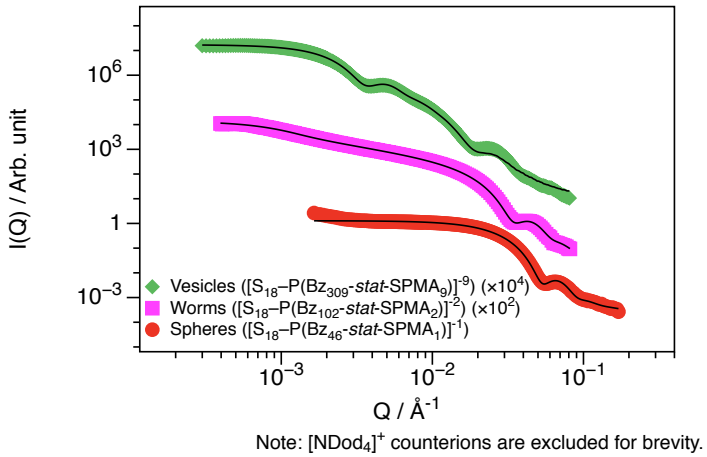

Fig. 3 SAXS data from [PSMA$_{18}$–P(BzMA$_y$-*stat*-SPMA$_z$)]$^{-z}\cdot z$[NDod$_4$]$^+$ diblock copolymer nano-objects in diluted to 1 wt. % in *n*-dodecane. Model fits to pure morphologies are shown and are described in the ESI.† Data are offset for clarity. The corresponding diblock copolymer compositions are given in the legends. Well-defined, pure spheres, worms, and vesicles are obtained for the specified diblock copolymer compositions.

To fully appreciate the significance of the ability to access higher-order morphologies for [PSMA$_{18}$–P(BzMA$_y$-*stat*-SPMA$_z$)]$^{-z}\cdot z$[NDod$_4$]$^+$ copolymer nano-objects as shown in Figure 2, we emphasize that the analogous PSMA$_{18}$–PBzMA$_y$ diblock copolymer nano-objects can only form kinetically-trapped spheres. Hence, these higher-order morphologies (worms and vesicles, for instance) are not produced simply because of the large molecular volume of the [NDod$_4$]$^+$[SPMA]$^-$ comonomer repeat units. This anionic comonomer does increase the volume of the structure-directing block. However, this alone is insufficient to drive the formation of non-spherical morphologies at this copolymer concentration. If it were, the same could be achieved by simply targeting a sufficiently long PBzMA block.

3.2 Effect of copolymer concentration

A series of PSMA$_{18}$–PBzMA$_y$ spheres was synthesized in *n*-dodecane at concentrations ranging from 20 to 40 wt. %. The d_Z values determined by DLS for dilute copolymer dispersions are shown in Figure 4, along with a representative TEM micrograph in each case. To compare *Z*-average diameters properly requires that the dispersion have a monomodal distribution and that particles are nearly-spherical in shape.[53] The intensity-weighted size distributions for the dispersions in Figure 4 meet these requirements and are shown in the ESI (Figure S1).† For spheres synthesized at 20 wt. %, the DLS diameters agree almost perfectly with literature data previously reported for PSMA$_{18}$–PBzMA$_y$ spheres in mineral oil,[28] with diameters (d_Z) that depend on the DP as a power law (with exponent $\alpha = 0.61$). This suggests that the structure-directing block is similarly segregated in both *n*-dodecane and in mineral oil at this concentration (20 wt. %).

For PSMA$_{18}$–PBzMA$_y$ nano-objects prepared at higher copolymer concentrations, the DLS diameters clearly differ from that expected for spheres, as indicated by the non-power law dependence on DP. This agrees with the TEM micrographs, which clearly show the presence of non-spherical morphologies. A recent literature report supports this observation. Poly(2-(methacryloyloxy)ethyl oleate)-stabilized PBzMA nano-objects synthesized via PISA in *n*-heptane form various morphologies depending on the copolymer concentration.[30] Specifically, worms are formed at 25 wt. %, but only spheres are formed at either 5 or 10 wt. %.[30] Similar observations have been made by Lopez-Olivia *et al*. for the PISA synthesis of polydimethylsiloxane–PBzMA diblock copolymer nano-objects in *n*-heptane.[27]

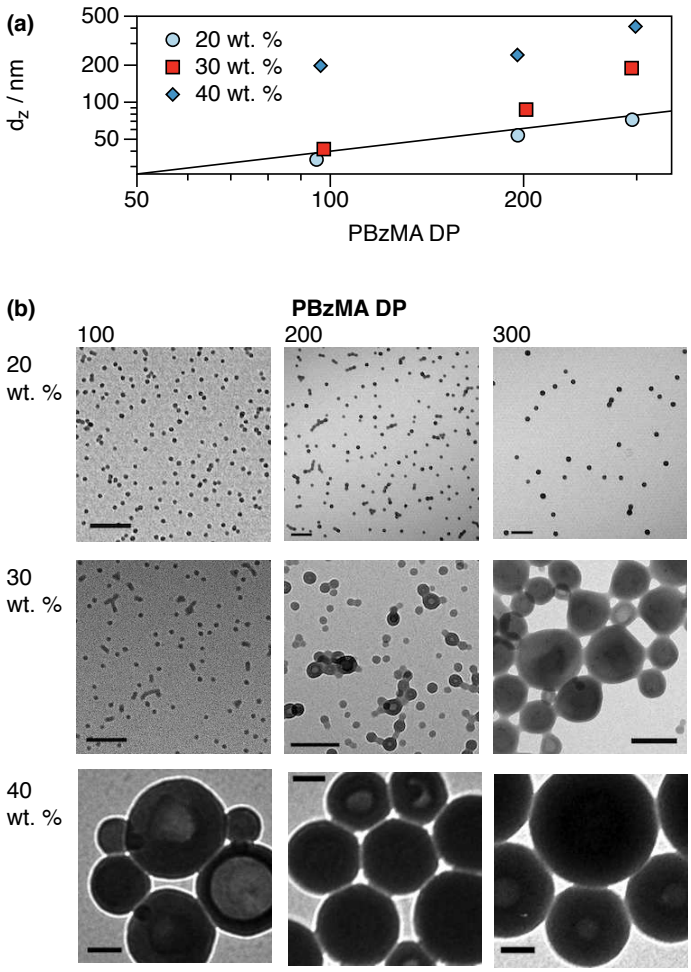

Fig. 4 The relationship between (a) DLS diameter (d_Z) and structure-directing PBzMA block DP for a series of PSMA$_{18}$–PBzMA$_y$ nano-objects in *n*-dodecane prepared at various copolymer concentrations. At 20 wt. %, the mean diameter conforms to that expected for only spheres and agrees well with literature data.[28] At higher copolymer concentrations, the marked increase in apparent particle diameter suggests the formation of non-spherical, possibly vesicular, morphologies. This agrees with the corresponding TEM micrographs (b). The power law of d_Z as a function of DP plotted in (a) is taken from Derry *et al*. for a comparable PSMA stabilizer.[28] Scale bars are 200 nm in each case.

This suggests that introducing the anionic monomer promotes access to non-spherical morphologies. The paradigm of

View Article Online
DOI: 10.1039/D0PY00101E

kinetically-trapped spheres can be broken at lower concentrations than is possible for PSMA–PBzMA nano-objects. Although the molecular volume of a $[NDod_4]^+[SPMA]^-$ repeat unit is greater than that of a BzMA repeat unit, this difference in volume alone is insufficient to drive the formation of non-spherical morphologies. At 20 wt. %, no $PSMA_{18}$-$PBzMA_y$ diblock copolymer can to form anything other than spheres, regardless of y.

To test this hypothesis, a series of diblock copolymer nano-objects was synthesized using a longer $PSMA_{34}$ macro-CTA. This should provide a more efficient steric stabilizer and, hence, favor the formation of spheres.[8,10] Moreover, this $PSMA_{34}$ macro-CTA is comparable to the one employed by Derry *et al.*, which enables a comparison to be made between this new series of $PSMA_{34}$ nano-objects with those reported in the literature.[28] For the $PSMA_{31}$–$PBzMA_y$ spheres reported by Derry *et al.*,[28] the power law exponent α was 0.50, which corresponds to unperturbed chains.[54,55] A series of $PSMA_{34}$–$PBzMA_y$ diblock copolymer nano-objects was synthesized in *n*-dodecane under the same conditions as those described in Figure 4, and DLS *Z*-average diameters are shown in Figure 5. As before, the power law shown in Figure 5 is taken from Derry *et al.*[28] It was not fitted to the new data that we present here. The power law relationship between DP and d_Z indicates the formation of spherical nano-objects, which is confirmed by the TEM micrographs shown in Figure 5.

To examine whether incorporation of the anionic comonomer can drive the formation of non-spherical morphologies in a system that does not exhibit any change in morphology with concentration, a series of $[PSMA_{18}–P(BzMA_y\text{-}stat\text{-}SPMA_z)]^{-z} \cdot z[NDod_4]^+$ diblock copolymer nano-objects was synthesized via PISA at 20 wt. %. Such nano-objects provide a useful comparison to those shown in Figure 2, with the only difference being the DP of the PSMA stabilizer block. A morphology map constructed by systematic variation of the core-forming block DP and mole fraction of anionic comonomer is shown in Figure 6. Only spheres are obtained in this case, unless the mole fraction of anionic comonomer is relatively high, which results in the formation of large, ill-defined compound micelles.

4 Conclusions

A new approach for controlling the morphology of diblock copolymer nano-objects prepared by RAFT-mediated PISA in non-polar media is reported. Previously, systematic variation of the structure-directing block DP usually provided the full range of copolymer morphologies expected (spheres, worms, or vesicles) provided that the steric stabilizer block was sufficiently short for efficient sphere-sphere fusion to occur on the time scale of the PISA synthesis. We show that statistical copolymerization of an ionic comonomer with BzMA enables the production of spheres, worms, and vesicles in *n*-dodecane at a copolymer concentration of 20 wt. %. In contrast, only kinetically-trapped spheres were obtained for PISA syntheses performed under the same conditions in the absence of this ionic comonomer, regardless of the target core-forming block DP. Thus the unexpected access to worms and vesicles cannot be simply attributed to a the greater volume of the structure-directing block.

In summary, incorporation of an ionic comonomer into the

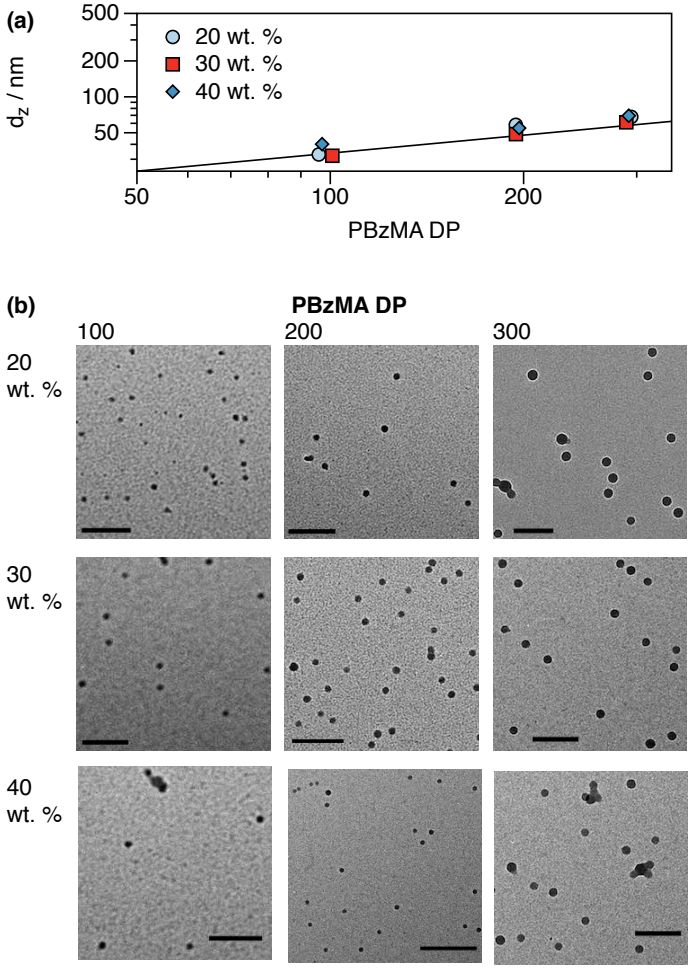

Fig. 5 The relationship between (a) DLS diameter (d_Z) and structure-directing PBzMA block DP for a series of $PSMA_{34}$–$PBzMA_y$ diblock copolymer nano-objects in *n*-dodecane prepared at various copolymer concentrations. The *Z*-average diameters are consistent with the formation of spheres and are in good agreement with literature data reported for a comparable $PSMA_{31}$–$PBzMA_y$ diblock copolymer series.[28] This agrees with the corresponding TEM micrographs (b). The power law of d_Z as a function of DP plotted in (a) is taken from Derry *et al.* for a comparable PSMA stabilizer.[28] Scale bars are 200 nm in each case.

View Article Online
DOI: 10.1039/D0PY00101E

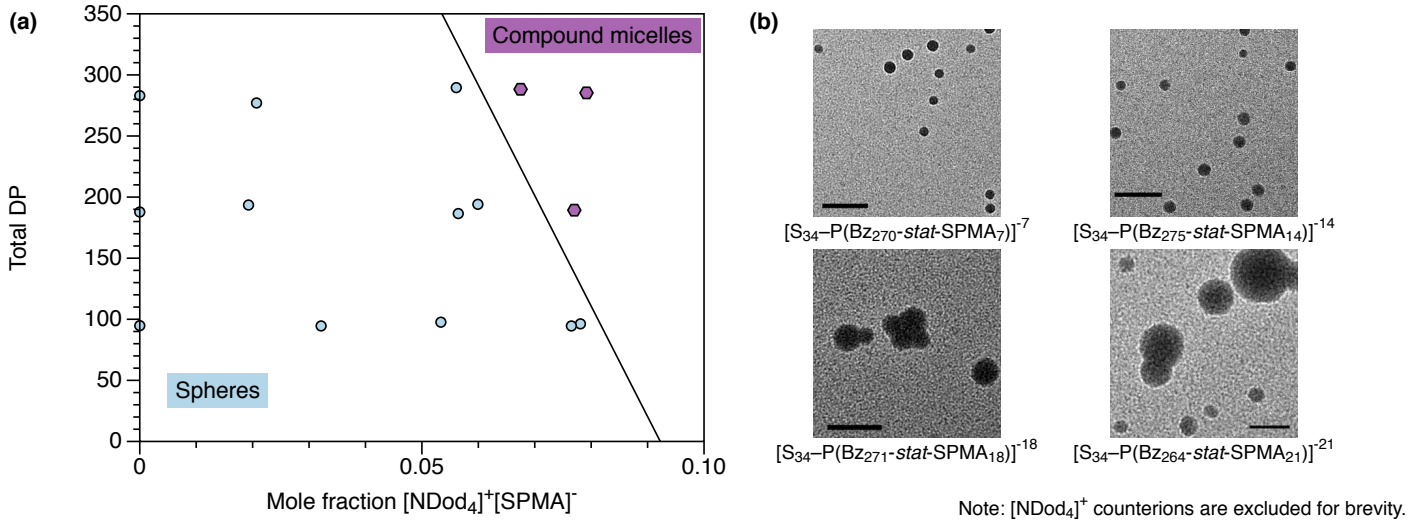

Fig. 6 Morphology map constructed for $[PSMA_{34}–P(BzMA_y\text{-}stat\text{-}SPMA_z)]^{-z} \cdot z[NDod_4]^+$ diblock copolymer nano-objects prepared in *n*-dodecane at 20 wt. %. Unlike the diblock copolymer nano-objects prepared using the $PSMA_{18}$ stabilizer, only spheres are obtained under most conditions. At higher mole fractions of anionic comonomer, relatively large, ill-defined nano-objects are obtained when targeting higher DPs. Representative TEM micrographs for spheres and compound micelles are shown. Scale bars are 200 nm in each case.

insoluble, structure-directing block enables the paradigm of kinetically-trapped spheres to be broken, at least for PISA syntheses conducted in non-polar media. It appears that the relatively large volume of the anionic comonomer, which forms an ion pair with its cationic counterion in *n*-dodecane, modifies the packing parameter, enabling access to higher-order, non-spherical copolymer morphologies. However, this unexpected observation is currently not well-understood. Future work varying the copolymer concentration (which has been shown to impact the morphologies formed in non-polar solvents[30]), the way the radical reaction is initiated, photoinitiation or thermal initiation (which will determine the reaction conditions and is known to impact the morphologies that form due to loss of end groups[56]), or the temperature of the reaction or its duration (which will impact the balance of the propagation reaction and the ion pair lifetime) are possible ways to explore the origin of this effect. As many characteristics of PISA are universal between water, alcohols, and non-polar solvents, these results will be relevant to more than just those interested in low dielectric fluids, and understanding its cause and how to apply the approach to other media clearly warrants further investigation.

Conflicts of interest

There are no conflicts to declare.

Acknowledgements

SPA acknowledges the ERC for a five-year Advanced Investigator grant (PISA 320372) and EPSRC (EP/J007846). The ESRF is acknowledged for awarding beamtime on ID02, and Diamond Light Source is acknowledged for awarding time on I22. The UK Science and Technologies Facility Council (STFC) is acknowledged for funding travel costs associated with visiting the ESRF and Diamond Light Source. The beamline staff at ID02 (ESRF, local contact Sylvain Prévost) and I22 (Diamond Light Source, local contact Andrew J. Smith) are acknowledged for support during measurements at the facilities.

Notes and references

1 *Amphiphilic Block Copolymers: Self-Assembly and Applications*, ed. P. Alexandridis and B. Lindman, Elsevier, Amsterdam, 2000.
2 Z. Gao, S. K. Varshney, S. Wong and A. Eisenberg, *Macromolecules*, 1994, **27**, 7923–7927.
3 L. Zhang and A. Eisenberg, *Science*, 1995, **268**, 1728–1731.
4 L. Zhang and A. Eisenberg, *J. Am. Chem. Soc.*, 1996, **118**, 3168–3181.
5 J. N. Israelachvili, D. J. Mitchell and B. W. Ninham, *J. Chem. Soc., Faraday Trans. 2*, 1976, **72**, 1525–1568.
6 J. Israelachvili, *Colloids Surf. A: Physicochem. Eng. Aspects*, 1994, **91**, 1–8.
7 B. Charleux, G. Delaittre, J. Rieger and F. D'Agosto, *Macromolecules*, 2012, **45**, 6753–6765.
8 N. J. Warren and S. P. Armes, *J. Am. Chem. Soc.*, 2014, **136**, 10174–10185.
9 J. Rieger, *Macromol. Rapid Commun.*, 2015, **36**, 1458–1471.
10 S. L. Canning, G. N. Smith and S. P. Armes, *Macromolecules*, 2016, **49**, 1985–2001.
11 M. J. Derry, L. A. Fielding and S. P. Armes, *Prog. Polym. Sci.*, 2016, **52**, 1–18.
12 A. B. Lowe, *Polymer*, 2016, **106**, 161–181.
13 J. Yeow and C. Boyer, *Adv. Sci.*, 2017, **4**, 1700137.
14 U. Tritschler, S. Pearce, J. Gwyther, G. R. Whittell and I. Manners, *Macromolecules*, 2017, **50**, 3439–3463.
15 N. J. W. Penfold, J. Yeow, C. Boyer and S. P. Armes, *ACS Macro Lett.*, 2019, **8**, 1029–1054.

View Article Online
DOI: 10.1039/D0PY00101E

16 A. Blanazs, S. P. Armes and A. J. Ryan, *Macromol. Rapid Commun.*, 2009, **30**, 267–277.
17 A. Blanazs, A. J. Ryan and S. P. Armes, *Macromolecules*, 2012, **45**, 5099–5107.
18 E. R. Jones, M. Semsarilar, P. Wyman, M. Boerakker and S. P. Armes, *Polym. Chem.*, 2016, **7**, 851–859.
19 L. A. Fielding, M. J. Derry, V. Ladmiral, J. Rosselgong, A. M. Rodrigues, L. P. D. Ratcliffe, S. Sugihara and S. P. Armes, *Chem. Sci.*, 2013, **4**, 2081–2087.
20 M. J. Derry, L. A. Fielding and S. P. Armes, *Polym. Chem.*, 2015, **6**, 3054–3062.
21 D. H. Napper, *Polymeric Stabilization of Colloidal Dispersions*, Academic Press, London, 1983.
22 A. Blanazs, J. Madsen, G. Battaglia, A. J. Ryan and S. P. Armes, *J. Am. Chem. Soc.*, 2011, **133**, 16581–16587.
23 L. Houillot, C. Bui, M. Save, B. Charleux, C. Farcet, C. Moire, J.-A. Raust and I. Rodriguez, *Macromolecules*, 2007, **40**, 6500–6509.
24 L. Houillot, C. Bui, C. Farcet, C. Moire, J.-A. Raust, H. Pasch, M. Save and B. Charleux, *ACS Appl. Mater. Interfaces*, 2010, **2**, 434–442.
25 J.-A. Raust, L. Houillot, M. Save, B. Charleux, C. Moire, C. Farcet and H. Pasch, *Macromolecules*, 2010, **43**, 8755–8765.
26 L. A. Fielding, J. A. Lane, M. J. Derry, O. O. Mykhaylyk and S. P. Armes, *J. Am. Chem. Soc.*, 2014, **136**, 5790–5798.
27 A. P. Lopez-Oliva, N. J. Warren, A. Rajkumar, O. O. Mykhaylyk, M. J. Derry, K. E. B. Doncom, M. J. Rymaruk and S. P. Armes, *Macromolecules*, 2015, **48**, 3547–3555.
28 M. J. Derry, L. A. Fielding, N. J. Warren, C. J. Mable, A. J. Smith, O. O. Mykhaylyk and S. P. Armes, *Chem. Sci.*, 2016, **7**, 5078–5090.
29 M. J. Derry, O. O. Mykhaylyk and S. P. Armes, *Angew. Chem. Int. Ed.*, 2017, **56**, 1746–1750.
30 B. Maiti, K. Bauri, M. Nandi and P. De, *J. Polym. Sci. A: Polym. Chem.*, 2017, **55**, 263–273.
31 G. N. Smith, L. L. E. Mears, S. E. Rogers and S. P. Armes, *Chem. Sci.*, 2018, **9**, 922–934.
32 M. J. Derry, O. O. Mykhaylyk, A. J. Ryan and S. P. Armes, *Chem. Sci.*, 2018, **9**, 4071–4082.
33 M. J. Derry, T. Smith, P. S. O'Hora and S. P. Armes, *ACS Appl. Mater. Interfaces*, 2019, **11**, 33364–33369.
34 Y. Pei, L. Thurairajah, O. R. Sugita and A. B. Lowe, *Macromolecules*, 2015, **48**, 236–244.
35 Y. Pei, J.-M. Noy, P. J. Roth and A. B. Lowe, *J. Polym. Sci. A: Polym. Chem.*, 2015, **53**, 2326–2335.
36 Y. Pei, O. R. Sugita, L. Thurairajah and A. B. Lowe, *RSC Adv.*, 2015, **5**, 17636–17646.
37 L. P. D. Ratcliffe, B. E. McKenzie, G. M. D. L. Bouëdec, C. N. Williams, S. L. Brown and S. P. Armes, *Macromolecules*, 2015, **48**, 8594–8607.
38 V. J. Cunningham, S. P. Armes and O. M. Musa, *Polym. Chem.*, 2016, **7**, 1882–1891.
39 S. L. Canning, V. J. Cunningham, L. P. D. Ratcliffe and S. P. Armes, *Polym. Chem.*, 2017, **8**, 4811–4821.
40 E. J. Cornel, S. van Meurs, T. Smith, P. S. O'Hora and S. P. Armes, *J. Am. Chem. Soc.*, 2018, **140**, 12980–12988.
41 G. N. Smith, M. J. Derry, J. E. Hallett, J. R. Lovett, O. O. Mykhaylyk, T. J. Neal, S. Prévost and S. P. Armes, *Proc. R. Soc. London A: Math., Phys. Eng. Sci.*, 2019, **475**, 20180763.
42 P. J. Docherty, M. J. Derry and S. P. Armes, *Polym. Chem.*, 2019, **10**, 603–611.
43 I. D. Morrison, *Colloids Surf. A: Physicochem. Eng. Aspects*, 1993, **71**, 1–37.
44 L. D. Farrand, N. Greinert, J. H. Wilson, T. Bauer, C. Topping and S. Norman, *Particles for electrophoretic displays*, Patent US 2016/0137767 A1, 2016.
45 L. D. Farrand, C. Topping and S. Norman, *Particles for electrophoretic displays*, Patent US 2016/0177103 A1, 2016.
46 R. F. T. Stepto, *Pure Appl. Chem.*, 2009, **81**, 351 –353.
47 S. Harrisson, *Polym. Chem.*, 2018, **9**, 1366–1370.
48 M. Basham, J. Filik, M. T. Wharmby, P. C. Y. Chang, B. El Kassaby, M. Gerring, J. Aishima, K. Levik, B. C. A. Pulford, I. Sikharulidze, D. Sneddon, M. Webber, S. S. Dhesi, F. Maccherozzi, O. Svensson, S. Brockhauser, G. Náray and A. W. Ashton, *J. Synch. Rad.*, 2015, **22**, 853–858.
49 J. Ilavsky and P. R. Jemian, *J. Appl. Cryst.*, 2009, **42**, 347–353.
50 S. Sugihara, A. Blanazs, S. P. Armes, A. J. Ryan and A. L. Lewis, *J. Am. Chem. Soc.*, 2011, **133**, 15707–15713.
51 L. Zhang and A. Eisenberg, *Polym. Adv. Technol.*, 1998, **9**, 677–699.
52 N. J. Warren, O. O. Mykhaylyk, A. J. Ryan, M. Williams, T. Doussineau, P. Dugourd, R. Antoine, G. Portale and S. P. Armes, *J. Am. Chem. Soc.*, 2015, **137**, 1929–1937.
53 Malvern Instruments, *Dynamic Light Scattering: Common Terms Defined*, White Paper, 2011.
54 L. Leibler, *Macromolecules*, 1980, **13**, 1602–1617.
55 S. Förster, M. Zisenis, E. Wenz and M. Antonietti, *J. Chem. Phys.*, 1996, **104**, 9956–9970.
56 L. D. Blackman, K. E. B. Doncom, M. I. Gibson and R. K. O'Reilly, *Polym. Chem.*, 2017, **8**, 2860–2871.

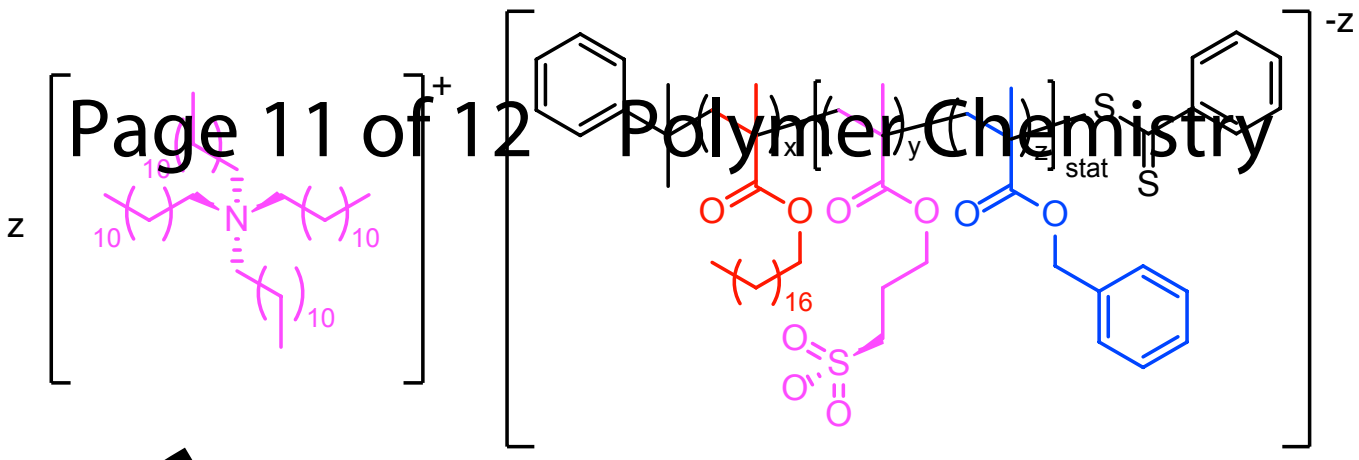

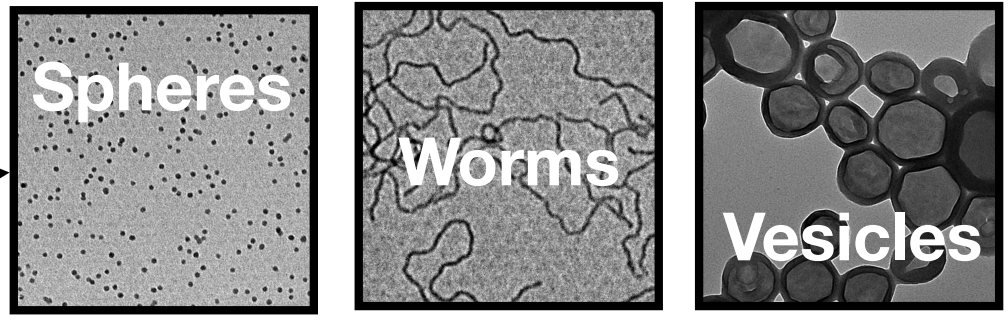

Varying degree of polymerization

Varying core monomer ratio

View Article Online
DOI: 10.1039/D0PY00101E

An ionic comonomer can cause a change in morphology to diblock copolymer nano-objects prepared by polymerization-induced self-assembly in a non-polar solvent that would otherwise form only spheres.